JAAS

Journal of Analytical Atomic Spectrometry

www.rsc.org/jaas

Volume 28 | Number 4 | April 2013 | Pages 413–614

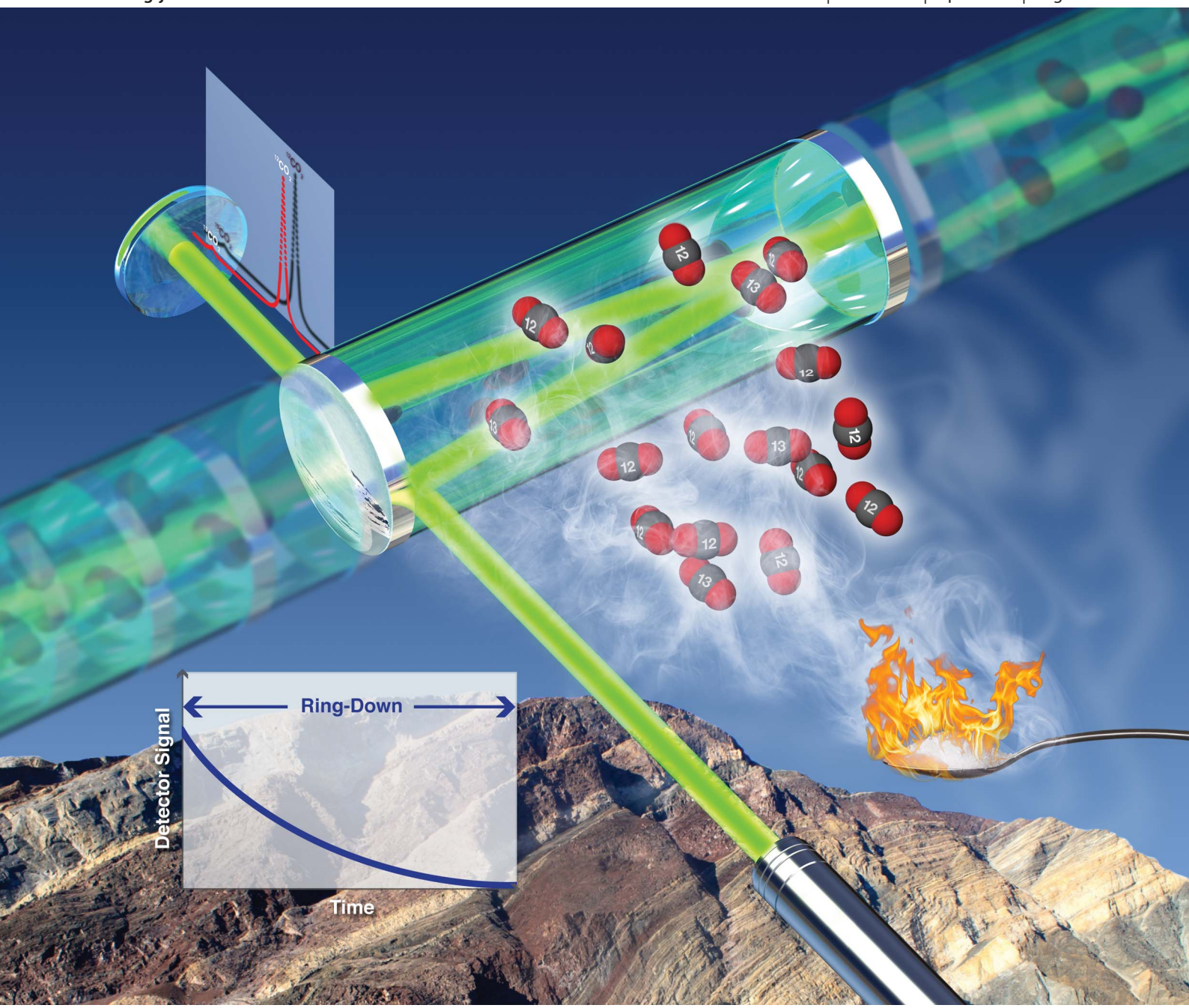

ISSN 0267-9477

RSC Publishing

PAPER

David Balslev-Clausen *et al*.

Precise and accurate $\delta^{13}C$ analysis of rock samples using Flash Combustion–Cavity Ring Down Laser Spectroscopy

JAAS

RSC Publishing

PAPER

Cite this: *J. Anal. At. Spectrom.*, 2013, **28**, 516

Precise and accurate $\delta^{13}C$ analysis of rock samples using Flash Combustion–Cavity Ring Down Laser Spectroscopy

David Balslev-Clausen,*[ab] Tais W. Dahl,[ac] Nabil Saad[d] and Minik T. Rosing[a]

Received 21st August 2012
Accepted 11th December 2012

DOI: 10.1039/c2ja30240c

www.rsc.org/jaas

The ratio of ^{13}C to ^{12}C in marine sedimentary rocks holds important clues to the evolution of the carbon cycle through Earth history. Isotopic analyses are traditionally carried out using isotope ratio mass spectrometry (IRMS), but this technique is labor-intensive, expensive and requires expert know-how. Here, we measure $^{13}C/^{12}C$ in natural sedimentary samples using Combustion Module–Cavity Ring Down Spectroscopy (CM-CRDS) with an average precision and a standard reproducibility of 0.05‰ and 0.2‰ (1 sd, $n = 17$), respectively. The accuracy of the technique was determined from certified reference compounds to be <0.3‰. This is comparable to the performance using routine laboratory mass spectrometry <0.11‰ (1σ). We report data from a Cambrian succession of organic-rich shales straddling a positive $\delta^{13}C_{org}$ excursion of 2‰. We conclude that the optical determination of bulk organic $\delta^{13}C$ provides a high performance alternative to routine laboratory mass spectrometry and is applicable for geochemical analyses.

1 Introduction

Isotopic analysis is an important tool applicable for a wide range of scientific disciplines. Currently, the primary tool for isotopic determination is ionization mass-spectrometry,[1] which requires skilled operation, high vacuum, and high maintenance. Over the past few years novel laser based methods have emerged and proven to be a competent alternative to mass spectrometry. These systems are simple to operate with a lower vacuum requirement and a lower cost of operation.

Stable isotope analyses of H, C, O, N and S are commonly used in geological, biological, environmental and medical sciences. This is because these elements in nature are both abundant and their isotopes fractionated. The sign and magnitude of fractionation can be used to trace chemical pathways in nature and governing physical parameters. For example, marine carbon cycle dynamics can be inferred from $\delta^{13}C$ in sedimentary rocks, and temperatures in the prehistoric climate can be derived from $\delta^{18}O$ and D/H in ice cores and sediments. Isotope compositions of all these major elements are now detectable with optical methods.[2–5] Precision, accuracy, and dynamic range are continuously improving as is the number of chemical species that can be determined.

Here, we investigate $^{13}C/^{12}C$ of organic carbon in geological materials using a flash combustion Cavity Ring Down Spectrometer system similar to that used by Graham *et al.*,[6] to show that optical isotope determination is a viable alternative to conventional mass spectrometry for geochemical purposes. We explore guidelines for optimal operation as well as limitations of the analyzer together with a direct comparison of the performance of existing techniques. We wish to inspire geochemists to use laser-based isotope techniques and continued improvement for the laser based tools in the future.

1.1 Principle of laser based detection

Cavity ring-down spectroscopy is a light absorption technique applying the Beer–Lambert's law, which states that the intensity of a light beam attenuates exponentially with distance, as it propagates through a light-absorbing medium. Optical methods provide high selectivity because different molecules absorb light of distinct wavelengths/frequencies. The narrow bandwidth of optical-frequencies in a tunable diode laser CRDS enables sampling of individual molecular species with insignificant interference from other species in the analyte gas. Also, the isotopologues of the molecular species (*e.g.* $^{16}O^{13}C^{16}O$ and $^{16}O^{12}C^{16}O$) are distinguishable with limited tailing or interferences from neighbouring molecular species, allowing measurement of isotopic ratios, through the individual isotopologue concentrations.

This CRDS utilizes three mirrors of very high reflectivity (~99.999%), which are aligned to form a closed optical path,

[a]*Natural History Museum of Denmark, University of Copenhagen, Øster Voldgade 5-7, DK-1350 København K, Denmark. E-mail: dbc@nbi.ku.dk; Tel: +45 3532 0042*

[b]*Centre for Ice and Climate, University of Copenhagen, Juliane Maries Vej 30, DK-2100 København Ø, Denmark*

[c]*Institute of Biology, University of Southern Denmark, Campusvej 55, 5230 Odense M, Denmark*

[d]*Picarro Inc., 3105 Patrick Henry Dr., Santa Clara, California 95054, USA*

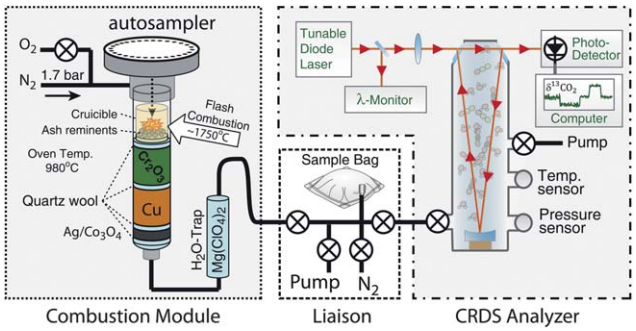

Fig. 1 Diagram of the CM-CRDS system. The high sensitivity of cavity ring-down optical absorption spectroscopy is used to quantify the $\delta^{13}C$ isotope composition of the CO_2 combustion product from a standard flash combustion module.

denoted as "the optical cavity", see Fig. 1. Laser light is coupled into this cavity through one of the mirrors and the light circulates in the closed path hundreds of thousand times, giving an effective absorption path length of more than ten kilometers for a gas cell only half a meter in size.

The absorptive losses in the cavity can be quantified in various ways, including Cavity Enhanced Absorption Spectroscopy (CEAS),[7] Integrated Cavity Leak-Out Spectroscopy (ICOS),[8] Optical Feedback CEAS (OF-CEAS)[9] and many others. Here we focus on CRDS.

With the high reflectivity of the mirrors, light is not simply transmitted in or out of the cavity. Only light which has a wavelength matching an integer fraction of the cavity round trip length provides a circumstance, where the tiny amount of light transmitted through the mirror coherently amplifies a high optical power in the cavity. When this resonance condition is met, light is emitted from the cavity and can be measured with a photo-detector (Fig. 1). The optical absorption losses in the cavity at the given frequency are quantified by $1/(\tau c)$ where c is the speed of light and τ is the exponential decay time (10's of μs) for the light leaking out of the cavity, when turning off the laser power (happens in <0.1 μs). By repeating this ring-down measurement over different frequencies the optical absorption spectrum is obtained. The magnitude of the absorption loss scales linearly with the isotopologue molar concentration. So by measuring two reference gases the instrument can be calibrated. Further details on the $\delta^{13}CO_2$ CRDS analyser are described by Crosson *et al.* in 2002.[10]

The primary advantage of the optical method is that it is a nondestructive measurement. In principle one could release a sample gas into the cavity cell, seal off the cell and either repeat the measurement as much as desired or recapture the sample and use it for other analytical purposes. Such efforts have been demonstrated for in-field greenhouse gas measurements of ice-core samples.[11]

2 Methods

2.1 CM-CRDS system

The laser analyser is a standard Cavity Ring-Down Spectrometer with combustion module (CM-CRDS) from Picarro Inc. A diagrammatic description of the system is shown in Fig. 1. The system consists of three parts: the combustion module, the Liaison interface, and the CRDS $\delta^{13}CO_2$ analyser.

2.1.1 Combustion module. The combustion module is a modified Costech Inc. Flash Combustion unit with an auto-sampler that runs up to 150 samples.

The samples are wrapped in tin-foil and placed in the auto-sampler. Each sample is introduced into the combustion tube one by one from the auto-sampler. Combustion proceeds in a quartz tube surrounded by a furnace controlled at 980 °C to within a few degrees. The combustion tube is packed with three catalysts, with a ceramic crucible atop of quartz wool, Cr(III)-oxide, quartz wool, copper wires, quartz wool, silvered cobalt oxide and another segment of quartz wool. The combustion furnace is continuously flushed at approximately 70 ml min^{-1} STP with a pure nitrogen carrier gas (99.9999% pure N_2). To burn the samples, a fixed volume of O_2 is introduced into the combustion furnace. The tinfoil wrap oxidizes at *ca.* 1700 °C, spurring the conversion of bulk carbon into gaseous CO_2. The combustion product is carried onward from the combustion furnace through a water trap (Magnesium Perchlorate) to the Liaison.

2.1.2 Liaison. The Liaison is a Picarro Inc. interface to the CRDS analyser. It consists of a valve manifold and three sample bags. The bags serve to deliver a steady flow of combustion product into the CRDS analyser. Each sample bag is flushed with pure N_2 (grade 6.0) and evacuated before each combustion product is collected in the bag. The combustion product is well mixed in the sample bag, so that a steady CO_2 concentration and carbon isotope mixture is observed when introduced into the CRDS analyser. Also, a stream of pure N_2 is introduced into the CRDS analyser to flush the CRDS cavity between each sample.

2.1.3 $\delta^{13}CO_2$ CRDS analyser. The CRDS analyser for $\delta^{13}CO_2$ measurements is a Picarro Inc. model G2121-i. The detection technique is described in Section 1.1. The CRDS analyser coordinates automated operation of the combustion module, Liaison, and data collection. The CRDS analyser continuously measures the gas in the cavity and reports a value for every 1 second.

2.2 IRMS system

The CM-CRDS technique is compared to state-of-the-art isotope ratio mass spectrometry, used for routine analyses of biological and geochemical materials. Here, we use a Thermo Scientific Delta V Advantage Continuous Flow Isotope Ratio Mass Spectrometer with a FLASH 2000 Element analyser to determine $\delta^{13}C$ in the samples. The front end of the instrument consists of an autosampler (MAS 200R), a Thermo NoBlank device, and a FLASH HT Plus combustion module connected to the mass spectrometer *via* a Conflo IV universal interface. The front end of the system is almost identical to the laser based instrument. Samples are introduced from the autosampler into the NoBlank, where the sample is parked and purged with He to reduce atmospheric CO_2 contamination. The sample falls into the combustion module where it is heated to 1020 °C. CO_2 is

produced along with other gaseous species (*e.g.* N_2 and H_2O) that are separated in a reducing environment of the combustion tube at 650 °C (the same principle as for CM-CRDS). The concentration of CO_2 is first measured with a Thermal Conductivity Detector (TCD) before it is mixed with a constant flow of He as the gas enters the mass spectrometer. Approximately 0.2 mg organic carbon (carbonate-free) was loaded into tin capsules, for the IRMS measurements. The sample throughput was ~5.2 samples per hour. The precision of the mass spectrometric $\delta^{13}C$ analysis is better than <0.11‰ (see Table 2).

3 Experimental

The performance of the CM-CRDS analyser was evaluated through the following six experiments. (1) Measuring the performance of the CRDS analyser without combustion front-end, using two bottled gasses with CO_2 concentrations at 0.4 ppm and 0.3%. (2) Repeatability and reproducibility of the CM-CRDS system for pure graphite samples. (3) Reproducibility for different sample compositions and matrices. (4) Oxidation efficiency of the flash combustion. (5) Comparison of the CM-CRDS method and CF-IRMS on multiple reference materials. (6) Application to geologic samples by measuring a stratigraphic section with a +2‰ isotope excursion and comparing CRDS to IRMS.

4 Materials

4.1 Reference materials

Four certified isotope standards and six in-house reference materials have been used for calibration and comparison of the mass spectrometer and laser spectrometer performances, listed in Table 1.

4.2 Geological samples

Geological samples were sub-sampled from the 28.9 meter long Andrarum-3 drill core housed at the Department of Geology, Lund University. The section comprises of mostly black to dark grey, finely laminated mudstones (shales) with early concretionary carbonate lenses (stinkstone or orsten) and a few primary carbonate beds.[12] The samples contain 5–15 wt% organic carbon and high pyrite Fe enrichments.[13] The sediments were deposited in the Mid- to Late Cambrian (Furongian) during the Streptoean Positive Carbon Isotope Event (SPICE). This marine event is recorded in carbonate rocks worldwide[14] and is manifested as a +2‰ shift in the organic carbon of the Andrarum-3 drill core. Ahlberg *et al.*, 2008 described the biostratigraphy and sedimentology in detail.[12] The shale samples were prepared at the Institute of Biology at University of Southern Denmark. First, rock samples were crushed in an agate mortar to <0.3 μm particles. Powders were then agitated for 2 hours in cold 2 M hydrochloric acid to remove carbonates and rinsed with de-ionized water to remove acid residuals. The carbonate-free samples were then dried and ground to a fine powder before weighing out in tin capsules.

5 Results and discussion

5.1 CRDS performance on bottled CO_2 mixtures

The precision of the CRDS analyser alone without front end was evaluated using two bottled mixtures of CO_2 in N_2, introduced directly into the CRDS analyser at constant flow. The low and high concentration mixtures were measured for 2 hours and 40 minutes, respectively, as shown in Fig. 2.

At a sample rate of 1 Hz, the precision of the $\delta^{13}C$ analysis (1 standard deviation) was 4.4‰ and 0.6‰ for concentrations at 373 and 2853 ppm, respectively. Standard errors of 0.4‰ and 0.03‰ were obtained with 7 minutes of data collection ($n = 420$) (Fig. 2). The precision improvement with averaging time was further evaluated using the Allan deviation, which quantifies the scatter of the mean values in consecutive time-intervals of the dataset.[15–18] It shows that the averaging improvement closely follows the optimal $1/\sqrt{n}$ relationship (dashed curves in Fig. 2) with n being the number of samples in the averaging window.

This test defines the optimal precision that can be achieved with the CM-CRDS. Additional uncertainty is induced during combustion and transfer to the detector in the combustion

Table 1 Reference materials applied in this study and their certified $\delta^{13}C$-isotope values referenced to the Vienna PeeDee Belemnite (V-PDB) scale

Name	Description	$\delta^{13}C_{V\text{-}PDB}$ (2σ)
USGS24[a,e]	Graphite	−16.05 ± 0.07
USGS40[a,e]	L-Glutamic acid	−26.39 ± 0.04
IVA_sed[b,e]	High organic sediment	−26.07 ± 0.13
IVA_prot[b,e]	Protein (casein)	−26.98 ± 0.13
IVA_urea[b,e]	Urea	−45.38 ± 0.17
CYC[b]	Cyclohexanone 2,4-dinitrophenylhydrazone, $C_{12}H_{14}N_4O_4$	
NIC[b]	Nicotinamide, $C_6H_6N_2O$	
ACT[b]	Acetanilide, C_8H_9NO	
AK99[c]	Activated carbon	
LEO[c]	Calcium carbonate	
NIS-1[c]	Graphite vein, Isua, W. Greenland	
PACS-2[d]	Marine sediment	

[a] US Geological Survey. [b] IVA Institut für Analysentechnik. [c] Univ. of Copenhagen. [d] National Research Council of Canada. [e] Certified value by corresponding agency.

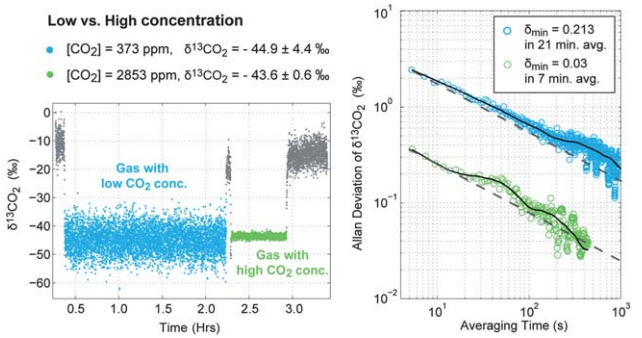

Fig. 2 CRDS measurements of bottled CO_2 mixed with N_2. Left: time sequence of measured delta values at 1 Hz sample rate. Right: Allan deviations calculated according to the highlighted data sections on the left plot.

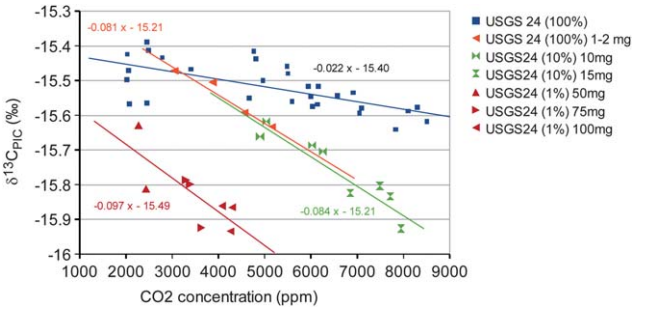

Fig. 4 Measured $\delta^{13}C$-values for pure graphite USGS-24 and in dilutions of 1% and 10% in highly pure quartz. Data in blue squares are discussed in Section 5.2 and the remaining data are discussed in Section 5.3.

module and Liaison interface. The analytical precision of a sample improves as a function of CO_2 concentration in the cavity and longer measuring time. The former was illuminated in the following experiment with pure graphite samples.

5.2 Repeatability on pure graphite

Pure graphite samples (USGS-24) were weighed out in various amounts and combusted in a completely new (unsaturated) reaction column. The 29 measured delta values are plotted *versus* the measured CO_2 concentration in Fig. 4 with blue squares. Values above 10 000 ppm and below 2000 were discarded due to detector saturation and low signal to noise ratio, respectively. For each of the measured samples, the one sigma standard error of the raw CRDS 1 Hz measurements was evaluated to determine the precision *versus* concentration shown in Fig. 3.

The precision of the CRDS analyser improves almost linearly with concentration, for CO_2 concentrations below 4000 ppm (Fig. 3). Above 4000 ppm, the precision is nearly constant at ~0.02‰. Therefore, this is the optimal precision that we can expect for repeated combustion experiments.

In Fig. 4 the 1σ (standard deviation) of the $\delta^{13}C$-value over all the 29 sample measurements is 0.07‰. The spread is 0.056‰ and 0.036‰ (1σ) below and above the median concentration of 5500 ppm, respectively. This is in agreement with the CRDS analysis improvement that we see for bottled gases in Fig. 3.

The linear fit through the data points in Fig. 4 indicates a concentration dependent on the $\delta^{13}C$-value of −0.02‰ per 1000 ppm of CO_2. The measured decrease of the $\delta^{13}C$-value with higher concentrations probably reflects that the lighter isotopes are preferentially converted into gas form. If we correct for this linear trend, then 1σ spreads are 40% reduced to 0.05‰, 0.03‰, and 0.02‰ for all data points, below and above 5500 ppm, respectively. This precision is comparable to the performance limit of the CRDS analyser. Thus, the observed isotope fractionation process is the only major source of additional imprecision in the instrument. The concentration dependent fractionation defines a maximum desirable sample load for the combustion column (Fig. 4) which in this case seems to fall between 5750 ppm and 6750 ppm.

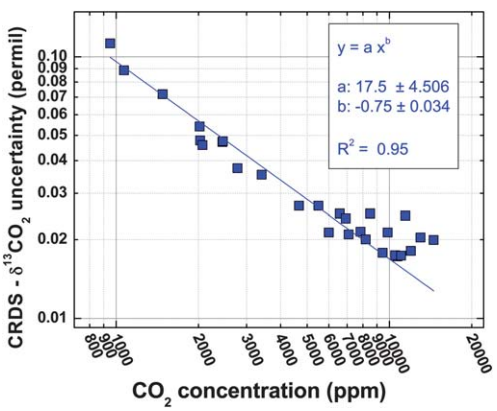

Fig. 3 Precision on measured $\delta^{13}C$ (1 standard error of mean) for individual samples of graphite (USGS-24) using a CM-CRDS.

5.3 Sample composition and matrix

Pure graphite (USGS-24) powder was diluted with high purity grade quartz powder to yield 1 and 10% carbon concentrations. Samples of the 1%, 10% and 100% graphite were weighed out in various doses to test the effect of sample composition. This experiment was not run under the unsaturated column conditions as for the measurements in Section 5.2 (blue squares). Still, the instrumental isotope fractionation for various matrix dilutions scales linearly with intensity, yet we observe significantly steeper concentration dependence of approximately −0.08‰ per 1000 ppm. The isotopic offset is negligible for the 10% mixture at 4000 ppm compared to pure graphite, while the 1% mixture show a significant offset of −0.4‰.

The results in Section 5.2 show that it is possible to reach the precision limit of the CRDS analyser, when applying the concentration correction with a pure graphite sample. Such a concentration correction is only valid to use if it applies to all materials of consideration. Unfortunately, this is not the case. Moreover, we have observed how the conditions of the combustion column may alter the sample response, and this is a serious drawback to the present design of flash combustion systems.

5.4 Combustion efficiency

The effect of combustion efficiency was tested by changing the O_2 dose injected at each combustion step. At a pressure of 0.85 bar, O_2 was loaded in one of four different loop volumes: 2.5 ml, 5 ml, 10 ml and 20 ml. Twelve samples of 15 ± 1 mg graphitic quartz veins with 13 wt% organic carbon were analyzed in triplicate for each O_2-loop volume. The combustion residual (*i.e.* uncombusted carbon remnant in the ash) was investigated by combusting empty tin capsules (four consecutive combustions of a single capsule) subsequent to the actual sample. The average results for the measurements of each oxygen-loop are shown in Fig. 5.

The combustion efficiency improves as more O_2 is introduced to the system. With the 2.5 mL O_2-loop only 40% of the carbon was combusted in the first flash cycle, and the remaining carbon is released during the consecutive cycles of empty tin-capsules. Notice that more carbon is actually released at the second flash cycle than in the first one. With 20 mL O_2, 97% of the carbon in the sample is combusted in the first flash combustion cycle.

To evaluate the isotopic consequences of incomplete combustion, we use Keeling's law of isotope mixing:[19]

$$\delta_m = \frac{c_b}{c_m}(\delta_b - \delta_S) + \delta_S \quad (1)$$

where c is the concentration (by atoms), δ is the isotope delta value, and subscripts S, b and m denote sample, background, and measured.

In the 20 mL O_2 experiment the initial combustion provided 6150 ppm CO_2 with $\delta^{13}C = -23.03 \pm 0.02‰$. The subsequent combustions of empty tin capsules provided a total of 220 ppm CO_2 with an isotopically distinct signature of $-20.8 \pm 0.20‰$. A correction for the lost heavy isotopes shows that the true $\delta^{13}C$ is $0.08 \pm 0.20‰$ higher than that recorded in the first combustion cycle. The large uncertainty is propagating from the low intensity measurements of the residual carbon. This measuring of subsequent blanks after each sample provides an option to correct for fractionation during incomplete combustion, but this is both time-consuming, labor-intensive and is dramatically increasing the uncertainty levels. If instead a sample, rather than an empty tin-capsule, is measured then the uncertainty issue of the subsequent isotope analysis is overcome, but unfortunately the matrix-dilution dependency on instrumental mass bias depends on too many unknown parameters, and this obscures the ability to reliably resolve the original sample composition (Fig. 4).

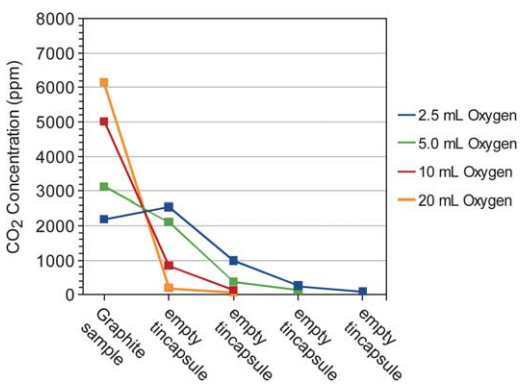

Fig. 5 Observed incomplete combustion of graphitic quartz vein in the CM-CRDS analyser. Measured CO_2 concentration at various O_2 loads (2.5 ml, 5 ml, 10 ml and 20 ml).

Running at high O_2 load improves combustion, but also increases the wear of the reduction catalyst. This CRDS analyser is designed for spectroscopy with a pure N_2 carrier. If the carrier is mixed with significant amounts of O_2, the accuracy of the isotope measurements may be compromised, because changing pressure broadening alters the absorption profiles. For oxygen removal, copper wires are installed in the column, and these wear out faster with increased O_2 levels. The above issues may be circumvented in the future by improving the spectroscopic method and/or by improving separation of a sample residue between combustion cycles.

5.5 Comparison of CM-CRDS and CF-IRMS

A comparison of the laser-based (CM-CRDS) and mass spectrometric method (CF-IRMS) was performed using known reference materials, summarized in Table 2. Three certified reference materials (USGS-40, USGS-24, and IVA_prot with $\delta^{13}C$ between −27 and −16‰) were used to calibrate both the CF-IRMS and CM-CRDS systems to the Vienna PeeDee Belemnite (V-PDB) scale.

Results for reference material measurements are summarized in Table 2. The analytical precision is presented as 1 standard deviation of four replicate analyses. Our data show that the precisions of nine reference materials are on average 0.07‰ and 0.04‰ for CRDS and IRMS, respectively. In four cases (IVA_prot, ACT, PACS-2 and AK99), the CRDS analysis was compromised by incomplete combustion recorded as >50 ppm CO_2 in the subsequent blank sample. Outliers of the IRMS data were discarded for analyses where the total carbon content deviated by >10% from the average content. Low intensity CRDS data were rejected for CO_2 concentration levels below 4000 ppm.

Fig. 6 shows the comparison of IRMS and CRDS data. The linear fit shows an excellent linear correspondence between the CRDS and IRMS data ($R^2 = 0.9986$). Although the linear fit is heavily weighted by the isolated $CaCO_3$ data point at +1.2‰, all points fall within the 85% prediction interval. Hence, a good linear correspondence between the datasets must be concluded for the full range from −32‰ to 1.2‰. The average $\delta^{13}C$ offset between the two techniques is 0.22‰ with a largest difference, 0.88‰, observed for active carbon (AK99).

5.6 Geological samples

The applicability of CRDS to geological materials was documented through blind test measurement using both the CM-CRDS and CF-IRMS systems. Black shale samples were taken from a Cambrian section with a positive $\delta^{13}C$ excursion from −30.5‰ to −28.1‰. The CRDS analysis was repeated six times on six different days, and the sample order was varied to explore

Table 2 $\delta^{13}C$ measurements obtained from direct comparison of CF-IRMS and CM-CRDS. The deviation gives the direct disagreement between the two measurements. Errors represent one standard deviation (1σ) of four replicate analyses

	Certified values (2σ)	CRDS (1σ)	IRMS (1σ)	Deviation (CRDS-IRMS)
USGS24	-16.05 ± 0.04	-16.06 ± 0.06	-16.06 ± 0.03	0.01
IVA_sed	-26.07 ± 0.13	-26.00 ± 0.08	-25.96 ± 0.11	-0.04
IVA_Prot	-26.98 ± 0.13	-27.04 ± 0.11	-27.08 ± 0.01	0.04
LEO		1.60 ± 0.11	1.21 ± 0.05	0.39
PACS-2		-23.80 ± 0.12	-23.18 ± 0.03	-0.62
AK99		-26.21 ± 0.03	-25.33 ± 0.04	-0.88
CYC		-26.89 ± 0.06	-26.20 ± 0.03	-0.69
NIC		-30.81 ± 0.04	-30.49 ± 0.01	-0.31
ACT		-27.73 ± 0.06	-27.84 ± 0.01	0.12

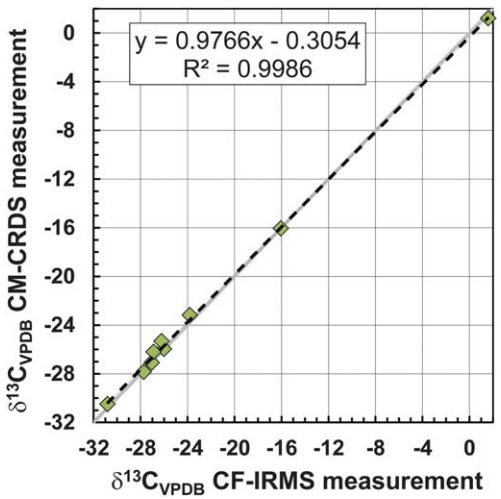

Fig. 6 Comparison of our CF-IRMS and CM-CRDS $\delta^{13}C$-measurements on 9 reference materials. The 1 : 1 line is shown in gray.

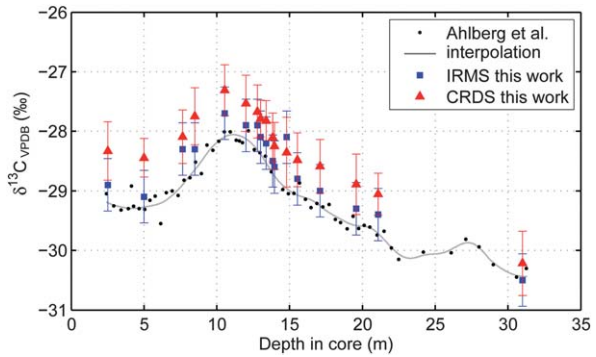

Fig. 7 Comparison of $\delta^{13}C$ measurements (2σ error bars) of the SPICE stratigraphic section through the Swedish Alum shale formation. Data are reported in Table 3. The systematic offsets between the curve obtained with CM-CRDS *versus* IRMS are in satisfactory agreement, because the applied CM-CRDS calibration for these measurements provides an additional 1‰ (1σ) to the uncertainty, which is not included to the plotted error bars.

potential cross-contamination (memory effect). We observe no systematic changes for the CM-CRDS system when data series is measured in the reverse order. The CM-CRDS measurements were calibrated to the V-PDB scale using USGS-24, USGS-40 and an in-house $CaCO_3$ reference. The sample from 2.5 m depth was measured at the beginning and end of each analytical session to monitor for daily drift. Yet, we observed no significant linear drift during the analytical sessions. For the CF-IRMS analyses, samples were measured only one day, but reference materials were measured repeatedly during subsequent sessions on different days. An in-house reference material (atropine) was run between samples to monitor for drift of the measured isotope ratio $^{13}C/^{12}C$. There was also no systematic drift with time, except in one session, where a linear drift correction of $-0.2‰$ magnitude could be applied over the 5 h course of the analyses ($R^2 = 0.97$, $n = 3$). Certified reference materials with $\delta^{13}C$ values between -45 and $-26‰$ (IVA-Sediment, IVA-Urea, IVA-Protein) were used to zero the ^{13}C scale to the V-PDB. These references were also used to determine the isotope composition of the three in-house standards (NIC, ACT, ATP).

The $\delta^{13}C$ data obtained for the shale samples using IRMS and CRDS are shown in Fig. 7 along with previously published IRMS data.[12] Clearly, both instruments capture the positive carbon isotope excursion preserved in the shales. The three datasets are compared in Fig. 8. The average reproducibility of the CRDS data is 0.25‰ (1σ). The accuracy of the IRMS data was estimated based on the average long term reproducibility of the standards listed in Table 2, being 0.24 permil (1σ).

The published data were obtained from samples in the same drill core taken at different depths.[12] Hence, a smoothed interpolation spline was made using a local regression with a weighted linear least squares and a 2nd degree polynomial model with a 20% window through Ahlberg's data points in order to compare with our measurements. The interpolated spline values are listed in Table 3 along with the CRDS and IRMS data. No error estimate was reported with Ahlberg's IRMS data, only the precision of the counting statistics of an in-house standard, NBS-19, was reported at $\delta^{13}C = 1.96 \pm 0.02‰$ ($n = 12$).[12] Hence, we assume that the uncertainty of Ahlberg's data is comparable to our IRMS data (0.24‰).

The optical and mass spectrometric techniques give absolute $\delta^{13}C$ values within the combined estimates. On average, CRDS is systematically offset from our IRMS data at +0.35‰ and Ahlberg's IRMS data fall $-0.31‰$ below.[12] All three datasets correlate positively with correlation coefficients $R^2 > 0.96$. The linear

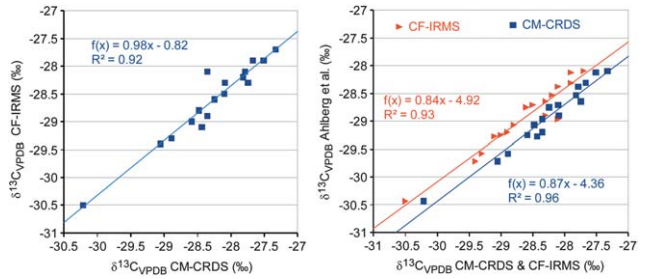

Fig. 8 Comparison of the three datasets from Fig. 7. The measurements of this work show better 1 : 1 correspondence than either of them do to the Ahlberg *et al.* record.

Table 3 $\delta^{13}C_{org}$ values of the Cambrian SPICE profile

Depth	Ahlberg *et al.*[a]	CF-IRMS[b]	CM-CRDS ± 1σ
2.51	−29.20	−28.9	−28.35 ± 0.22
5.00	−29.28	−29.1	−28.43 ± 0.19
7.65	−28.90	−28.3	−28.09 ± 0.26
8.50	−28.64	−28.3	−27.75 ± 0.27
10.54	−28.10	−27.7	−27.33 ± 0.24
12.00	−28.12	−27.9	−27.51 ± 0.27
12.8	−28.31	−27.9	−27.67 ± 0.26
13.00	−28.38	−28.1	−27.79 ± 0.18
13.40	−28.53	−28.2	−27.82 ± 0.19
13.85	−28.71	−28.5	−28.10 ± 0.23
13.97	−28.75	−28.6	−28.24 ± 0.23
14.81	−28.96	−28.1	−28.35 ± 0.34
15.53	−29.07	−28.8	−28.48 ± 0.26
17.10	−29.25	−29.0	−28.59 ± 0.26
19.57	−29.58	−29.3	−28.89 ± 0.29
21.09	−29.72	−29.4	−29.06 ± 0.20
31.06	−30.44	−30.5	−30.22 ± 0.31

[a] Interpolation values. [b] Average long term standard reproducibility (1σ) is 0.24‰.

regressions in Fig. 8 between the three datasets show that the CRDS measurements and the IRMS are in better agreement than the interpolated spline values from Ahlberg's curve. This deviation is primarily caused by a single sample at 30 m depth in the core. The two IRMS datasets are in agreement within the combined uncertainty $\sqrt{2} \times 0.24‰ = 0.34‰$, but there appears to be a systematic offset between the two curves. The offset between CRDS measurements and IRMS, at 0.35‰, also matches the slightly higher combined error of the CRDS-IRMS comparison. Ahlberg's curve was obtained using activated carbon (AK99) to zero at the V-PDB scale (B. Petersen, pers. communication). Our analysis shows that this reference material is also the hardest to reproduce (Table 2), and this may have contributed to the offset between the two IRMS curves. The CM-CRDS measurement accuracy is 1‰ (1σ) provided by the three reference materials applied[20] on the days of analysis (all having higher $\delta^{13}C$ values than the SPICE samples). Hence, the offsets between the curves can be reasonably ascribed to the applied reference materials, showing the importance of using certified reference materials with $\delta^{13}C$ values that span the full range of the samples.

6 Conclusion

The $\delta^{13}C$ of organic carbon and carbonate in powdered rock samples has been determined using a cavity ring-down spectrometer (CM-CRDS).

- The CM-CRDS laser based detection system allows for determination of $\delta^{13}C$ in reference materials, bulk organic carbon and carbonate rocks at a precision comparable to the CF-IRMS.
- The major source of error lies in the combustion front end for this type of isotope analysis and not with the type of detector in use.
- The sample need is slightly higher for CRDS (0.5–1.3 mg C) than for IRMS (0.2 mg C).
- $\delta^{13}C$ in bulk organic matter from the ~500 million year old Alum shale formation was accurately measured with both laser spectrometry and mass spectrometry. The magnitude and direction of the isotope excursion (+2‰) is captured within the combined error of analyses, 0.3‰.

We conclude that the new laser spectrometers already provide a competitive and high-precision alternative to routine laboratory mass spectrometry for carbon isotope determinations in geological materials.

Acknowledgements

We thank B. Buchardt and B. Petersen (Univ. Copenhagen) for sharing reference materials (LEO and AK99). We thank C. W. Antivakis, B. Thamdrup, D. E. Canfield and S. Crowe (Univ. of Southern Denmark) for assistance and fruitful discussions. We also thank D. D. Jensen and T. Blunier (Univ. of Copenhagen) for their support. TWD was sponsored by Villum Kann Rasmussen foundation. TWD, DBC and MR thank Danish National Research Foundation (Nordic Center for Earth Evolution) for financial support. DBC thank The Danish National Research Foundation (Center for Ice and Climate) and The Lundbeck foundation for financial support.

References

1 J. Sabine Becker, *J. Anal. At. Spectrom.*, 2005, **20**, 1173–1184.
2 E. Moyer, D. Sayres, G. Engel, J. St. Clair, F. Keutsch, N. Allen, J. Kroll and J. Anderson, *Appl. Phys. B: Lasers Opt.*, 2008, **92**, 467–474.
3 J. Mohn, C. Guggenheim, B. Tuzson, M. K. Vollmer, S. Toyoda, N. Yoshida and L. Emmenegger, *Atmos. Meas. Tech.*, 2010, **3**, 609–618.
4 L. E. Christensen, B. Brunner, K. N. Truong, R. E. Mielke, C. R. Webster and M. Coleman, *Anal. Chem.*, 2007, **79**, 9261–9268.
5 R. N. Zare, D. S. Kuramoto, C. Haase, S. M. Tan, E. R. Crosson and N. M. R. Saad, *Proc. Natl. Acad. Sci. U. S. A.*, 2009, **106**, 10928–10932.
6 W. M. Graham, R. H. Condon, R. H. Carmichael, I. D'Ambra, H. K. Patterson, L. J. Linn and F. J. Hernandez Jr, *Environ. Res. Lett.*, 2010, **5**, 045301.

7 I. Ventrillard-Courtillot, E. Sciamma O'Brien, S. Kassi, G. Mjean and D. Romanini, *Appl. Phys. B: Lasers Opt.*, 2010, **101**, 661–669.
8 P. Maddaloni, G. Gagliardi, P. Malara and P. D. Natale, *J. Opt. Soc. Am. B*, 2006, **23**, 1938–1945.
9 J. Morville, S. Kassi, M. Chenevier and D. Romanini, *Appl. Phys. B: Lasers Opt.*, 2005, **80**, 1027–1038.
10 E. R. Crosson, K. Ricci, B. Richman, F. Chilese, T. Owano, R. Provencal, M. Todd, J. Glasser, A. Kachanov, B. Paldus, T. Spence and R. Zare, *Anal. Chem.*, 2002, **74**, 2003–2007.
11 T. Blunier, J. Chappellaz, S. Schüpbach, C. Stowasser, R. Dallmayr, O. Pascual, M. Bigler and D. Leuenberger, *AGU Fall Meeting Abstracts*, 2010, p. D5.
12 P. Ahlberg, N. Axheimer, L. E. Bascook, M. E. Eriksson, B. Schmitz and F. Terfelt, *Lethaia*, 2009, **42**, 2–16.
13 T. W. Dahl, E. U. Hammarlund, A. D. Anbar, D. P. G. Bond, B. C. Gill, G. W. Gordon, A. H. Knoll, A. T. Nielsen, N. H. Schovsbo and D. E. Canfield, *Proc. Natl. Acad. Sci. U. S. A.*, 2010, **107**, 17911–17915.
14 B. C. Gill, T. W. Lyons, S. A. Young, L. R. Kump, A. H. Knoll and M. R. Saltzman, *Nature*, 2011, **469**, 80–83.
15 D. W. Allan and J. A. Barnes, *Proc. 35th Ann. Freq. Control Sympoium*, USARADCOM, Ft. Monmouth, NJ 07703, 1981.
16 F. Czerwinski, A. C. Richardson and L. B. Oddershede, *Opt. Express*, 2009, **17**, 13255–13269.
17 P. Werle, *Appl. Phys. B: Lasers Opt.*, 2011, **102**, 313–329.
18 P. Werle, R. Mücke and F. Slemr, *Appl. Phys. B: Lasers Opt.*, 1993, **57**, 131–139.
19 C. D. Keeling, *Geochim. Cosmochim. Acta*, 1958, **13**, 322–334.
20 D. Balslev-Clausen, Ph.D. thesis, Niels Bohr Institute, University of Copenhagen, 2011.